

Reaction of aluminum powder with water in cement-containing refractory castables

A.R. Studart^{a,*}, M.D.M. Innocentini^b, I.R. Oliveira^b, V.C. Pandolfelli^b

^a Department of Materials, Swiss Federal Institute of Technology (ETHZ), Zurich CH-8092, Switzerland

^b Department of Materials Engineering, Federal University of São Carlos, São Carlos, SP 13565-905, Brazil

Received 15 January 2004; received in revised form 28 June 2004; accepted 10 July 2004

Available online 28 August 2004

Abstract

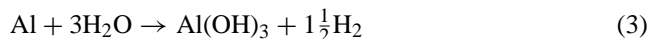
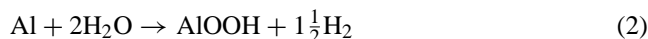
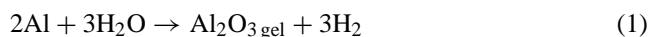
Aluminum powder is quite often used in refractory castables either to minimize explosive spalling during castable de-watering or to inhibit the oxidation of coke/graphite at high temperatures in carbon-containing materials. In the first case, the aluminum powder is expected to increase the permeability of castables by generating H₂ gas during reaction with H₂O and forming open porosity within the microstructure. In the latter application, on the other hand, it is desirable that a minimum amount of aluminum reacts with H₂O during castable processing, so that most of the metal remains in the microstructure to prevent carbon oxidation. Therefore, the understanding of the mechanisms involved in the Al–H₂O reaction in refractory castables is of crucial importance for an appropriate use of aluminum powder in either of these applications. This article aims at investigating the factors that determine the kinetics of the Al–H₂O reaction in cement-based castables. The chemistry of the castable aqueous solution was observed to play a major role on the kinetics of this reaction. A comprehensive qualitative model is proposed in the paper to describe the rate-limiting steps and the driving forces that trigger the Al–H₂O reaction in cement-based refractory castables. © 2004 Elsevier Ltd. All rights reserved.

Keywords: Al powder; Corrosion; Cement; Refractory castables; Castables

1. Introduction

Aluminum powder has been utilized for many years in the refractory industry either to prevent explosive spalling of castables during the de-watering process¹ or to avoid graphite/coke oxidation at high temperatures in carbon-containing refractories.² The role of the aluminum powder when used in carbon-based refractories is to act as a “sacrifice material” and be oxidized before the oxidation of carbon in O₂-rich environments. In the case of the de-watering process, aluminum powder is added to the castables to react with water and, by generating H₂ gas, to increase the refractory permeability. This is expected to facilitate the evaporation of water during drying and, thus, reduce the probability of spalling during castable de-watering.

A common feature of these applications is the need to control the reaction of aluminum powder with water during castable processing. In addition to H₂ gas, such reaction leads to the formation of alumina gel, boehmite (AlOOH) and/or gibbsite (Al(OH)₃), as follows³



For de-watering purposes, it is required that the aluminum extensively reacts with water to generate the H₂ gas responsible for opening permeable channels throughout the castable. In carbon-containing refractories, on the other hand, the aim is to inhibit the aluminum–water reaction so that a significant amount of the metal remains in the microstructure after castable processing. Therefore, the understanding

* Corresponding author.

E-mail address: andre.studart@mat.ethz.ch (A.R. Studart).

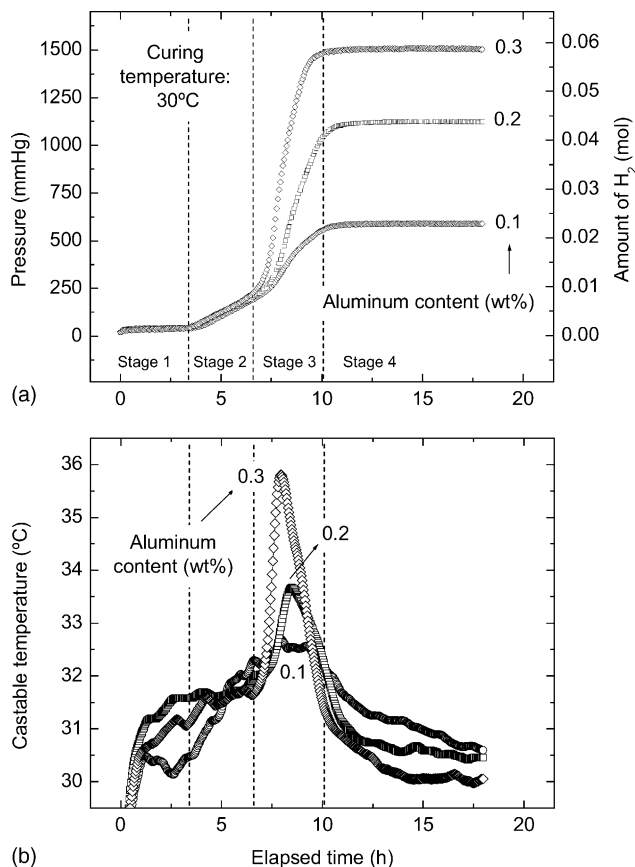


Fig. 1. (a) Pressure increase and amount of H₂ gas evolved as a function of time for castables containing different aluminum powder contents (grade 101/11-NR) at a curing temperature of 30°C. Graph (b) displays the temperature variations detected in the castables as a function of time.

of the kinetics of the above reactions under the processing conditions of castables (pH, temperature, ionic strength and species) is crucial for optimizing the use of aluminum powder either as a gas-generating additive or as inhibitor of carbon oxidation in refractory materials. Such knowledge would eventually allow us to control the Al reaction kinetics so that both functions can be accomplished in carbon-rich refractories.

Several factors that affect the aluminum–water reaction in refractory castables have been outlined by the authors in a recent paper.¹ The reaction was assessed by monitoring the pressure developed by Al-containing castables as a function of time, as depicted in Fig. 1. Due to the lack of model studies on this subject in the refractory field, these results were initially interpreted taking into account past investigations on the corrosion behavior of aluminum metal in water.^{4,5} The three main corrosion stages identified in these studies were attributed to the sequential formation of a boehmite (1st stage, slow rate) and a bayerite (2nd stage, highest rate) surface layer, followed by a long term corrosion stage (3rd stage, slow rate).⁵ It should be mentioned that in these investigations no major effect on the overall corrosion was attributed

to the impurities of the aluminum specimens (0.420% Fe, 0.085% Si, 0.006% Ca).⁵

The large similarity between the various corrosion stages of aluminum in water and the stages observed during H₂ generation in castables (Fig. 1) suggests that the aluminum–water reaction is governed by the same mechanism in both cases. However, a more detailed analysis of the kinetics of these processes reveals that the reaction of aluminum in the castables occurs markedly faster than that reported in the corrosion studies. It is important to note that these comparisons take into account the significant difference in surface area of the Al particles used in castables and the Al plates employed in corrosion investigations. The amount of aluminum reacted in the castables (in mol of Al/Al surface area), for instance, achieved levels as high as 3.7×10^{-5} mol/cm² after 10 h, whereas in the corrosion experiments only 1.3×10^{-5} mol/cm² of aluminum had reacted after a period of time as long as 100 days.^{1,5} This can be attributed to the maximum reaction rate of almost three orders of magnitude higher for the aluminum added to castables ($\sim 1.9 \times 10^{-5}$ mol/h cm²) in comparison to the aluminum used in the corrosion study ($\sim 7 \times 10^{-8}$ mol/h cm²).^{1,5} A more detailed discussion about the corrosion stages observed in the castables will be given in Section 3.4.

An extensive number of papers on aluminum corrosion have focused on the role of aggressive anions, particularly Cl⁻, on the corrosion behavior. After a thorough compilation of experimental findings reported in the literature, Foley⁶ suggested that the Al corrosion process comprises the following sequential steps: (1) adsorption of the reactive anion on the oxide-covered aluminum, (2) chemical reaction of the adsorbed anion with the aluminum ion in the Al oxide/hydroxide surface lattice, (3) thinning of the oxide film by dissolution, and (4) direct attack of the exposed metal by the anion. According to Foley, the overall Al corrosion behavior is in most cases controlled by one of these sequential steps.⁶

Two special features differentiate the chemical environment found in cement-based refractory castables from that usually considered in Al corrosion investigations: the pH and the concentration of aggressive anions. In cement-based refractories the pH is markedly higher (>11) and the concentration of Cl⁻ is negligible in comparison to those usually reported in corrosion studies ($5 < \text{pH} < 8$, $0.1 \text{ N} < [\text{Cl}^-] < 1.0 \text{ N}$ typically). In this study, we aim at understanding how this different chemical environment affects the corrosion of Al powder, determining which of the above-mentioned steps controls the reaction Al–H₂O in cement-based refractory castables. This would allow us to identify the reasons for the faster rates and higher yields observed in castables in comparison to those reported for the corrosion of aluminum metal. The identification of the rate-limiting steps involved in the Al–H₂O reaction promises better use of aluminum powder either as a gas-generating agent or an inhibitor of carbon oxidation at high temperatures in refractory materials.

2. Materials and methods

2.1.1. Castable composition

The refractory castables prepared in this work consisted of 98 wt.% alumina (Alcoa Chemicals, USA; Alcoa Alumínio, Brazil) and 2 wt.% calcium aluminate cement (CA-14, Alcoa Chemicals, USA). Calcined aluminas ($d_p < 100 \mu\text{m}$, A1000 SG and A3000 FL) were used as matrix fine powders (22 wt.%), whereas white fused alumina of varying particle sizes (4.5 mm to $\sim 40 \mu\text{m}$, grades 4/10, 8/20, 10/36, 20/40 and 200F) were used as aggregates (76 wt.%).

The particle size distribution of the castable composition (Fig. 2) was adjusted to a theoretical curve, based on Andreason's packing model with a coefficient of distribution $q = 0.21$, in order to obtain potentially self-flow castables.^{7,8}

The aluminum powder investigated in this study (99.7% Al, 0.15% Fe, 0.13% Si, $d_{50} = 32 \mu\text{m}$, surface area = $0.07 \text{ m}^2/\text{g}$) was supplied by Alcoa Alumínio/Brazil in coated (with paraffin) and uncoated grades (101-R and 101/11-NR, respectively) and added to the dry composition in amounts ranging from 0.1 to 0.3 wt.%. The amount of impurities in the Al powder studied in this work is significantly lower than that reported in other investigations on aluminum corrosion.^{5,6} Therefore, these minor impurities are not expected to play a major role on the corrosion data obtained in our study.

Citric acid (anhydrous, Labsynth, Brazil) in previously optimized content (0.05 wt.%) was used as dispersing agent in all compositions.⁸ The castables were prepared by mixing water (4.52 wt.% dry basis) to the raw materials in a paddle mixer for approximately 5 min. The curing temperature ranged from 8 to 50 °C.

2.2. Measurement of evolved hydrogen

The amount of H_2 gas generated by the aluminum–water reaction was assessed by measuring the pressure developed inside a hermetic vessel in which 500 g of the Al-containing

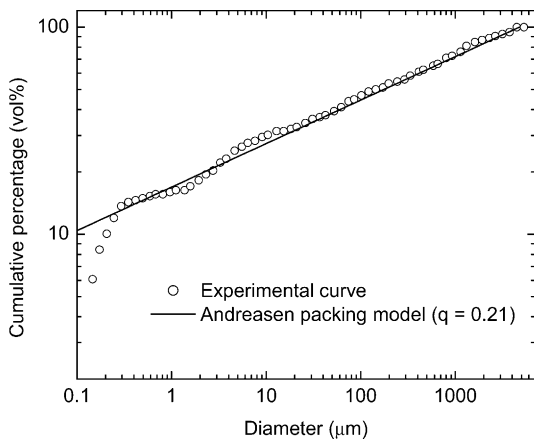


Fig. 2. Particle size distribution of the Al-containing castables prepared in this study.

castable was placed for curing. The sealed vessel was kept inside a water bath at a constant pre-set temperature. An electronic transducer monitored the pressure increase (ΔP) inside the vessel while two J-type thermocouples recorded the bath and the castable temperatures. Pressure and temperature data were gathered by computer at 10-s intervals until the pressure stabilized inside the vessel.

The amount of H_2 produced by the aluminum–water reaction (n_{H_2}) was calculated from the measured ΔP values (in mmHg), using the ideal gas law

$$n_{\text{H}_2} = \frac{\Delta P V_V}{RT} \quad (4)$$

where V_V is the free volume of the vessel (0.738 L), T is the curing temperature and R is the universal constant of gases ($62.36 \text{ mmHg L mol}^{-1} \text{ K}^{-1}$).

3. Results and discussion

3.1. Effect of cement

The presence of calcium aluminate cement in the refractory castables leads to significant changes in the chemistry of the interparticle aqueous solution and may, therefore, also affect the reaction between aluminum powder and water.

When in contact with water, cement particles start to dissolve yielding Ca^{2+} and $\text{Al}(\text{OH})_4^-$ ions, leading to an increase of the pH and the ionic strength of the aqueous medium.⁹ After a certain period of time, the dissolved species achieve a super-saturation level in the aqueous solution, which persists until nuclei of calcium aluminate hydrates are formed. The nucleated hydrates are then rapidly grown, causing a marked decrease in the concentration of Ca^{2+} and $\text{Al}(\text{OH})_4^-$ ions in the liquid medium (Fig. 3).

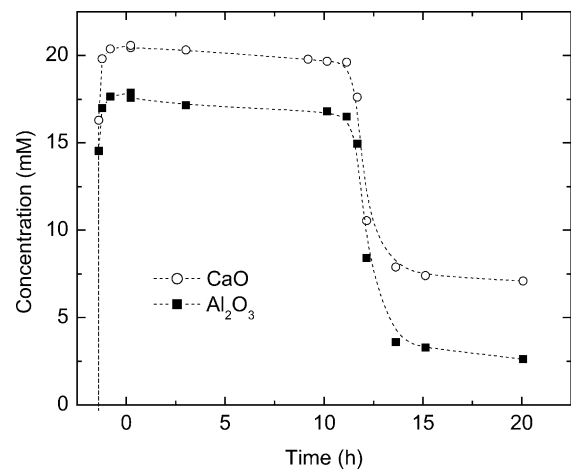


Fig. 3. Typical concentration of Ca^{2+} and $\text{Al}(\text{OH})_4^-$ ions in aqueous solution during cement dissolution and precipitation processes (graph adapted from Barret et al.⁹). The Ca^{2+} and $\text{Al}(\text{OH})_4^-$ ions are represented in the graph as the respective oxides CaO and Al_2O_3 , which leads to the following concentration ratios: $[\text{Ca}^{2+}]:[\text{CaO}]$ and $[\text{Al}(\text{OH})_4^-]:2[\text{Al}_2\text{O}_3]$.

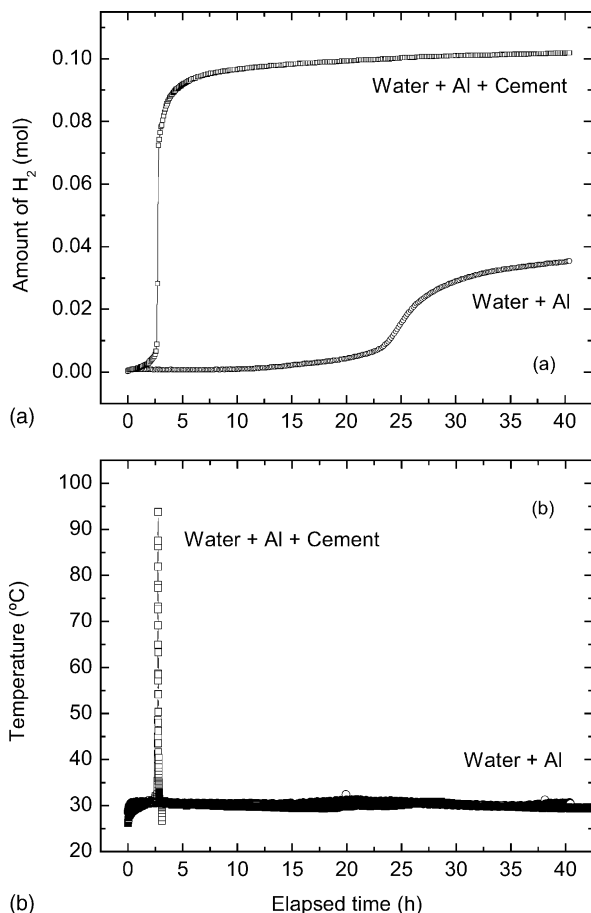


Fig. 4. (a) Amount of H₂ evolved and (b) temperature increase observed for aluminum-containing suspensions (grade 101-R) either in the presence or absence of cement (curing temperature: 30 °C). Similar results are expected for suspensions containing the uncoated aluminum powder grade (101/11-NR).

The effect of the dissolution/precipitation process of cement on the Al–H₂O reaction was evaluated by performing a set of experiments with suspensions containing only aluminum powder and water either in the presence or absence of cement. These suspensions were prepared using the same amount of aluminum powder, water and cement required for the preparation of 500 g of castable (1.5, 22.3 and 10 g, respectively).

Fig. 4 shows that the Al–H₂O reaction occurs much earlier and faster in the presence of cement than in its absence. A marked temperature increase was observed in the cement-containing suspension concurrently to the evolution of H₂, whereas no temperature change was detected in the suspension containing only aluminum and water. Additionally, only 42% of the aluminum present in the suspension without cement was reacted after 40 h of experiment, in contrast to the almost complete (95%) reaction of aluminum in the cement-containing composition. This indicates that the presence of cement has a decisive effect on the aluminum–water reaction and probably accounts for the discrepancies observed between the results obtained in cement-based castables (Fig. 1) and those found in literature for the corrosion of aluminum.⁵

Once the effect of cement has been confirmed, the main issue is then to understand how the chemical environment developed during the dissolution/precipitation process of cement (Fig. 3) influences the Al–H₂O reaction.

Due to their spontaneous and highly exothermic nature, the reactions (1)–(3) are not expected to be the kinetics-controlling step of the overall mechanism of H₂ generation. Instead, the overall reaction rate is often controlled by the thin aluminum hydroxide layer rapidly formed around the aluminum particles as a result of these reactions. This thin surface hydroxide layer tends to prevent the aluminum from being further oxidized by the water molecules, leading to the usually high corrosion resistance of aluminum metal. Therefore, in order to determine the effect of Ca²⁺ and Al(OH)₄[−] dissolved ions, as well as the precipitated hydrates, on the kinetics of the Al reactions, one has to understand how these species interact with the hydroxide protective layer.

Previous studies have shown that the presence of such protective layer may not be enough to avoid the corrosion of aluminum parts used, for instance, in coolant circuits of nuclear power reactors.⁵ One of the hypotheses for the corrosion of aluminum in such application is that the aluminum hydroxide protective layer is gradually dissolved into the aqueous solution, allowing the water molecules to corrode the inner aluminum metal. The dissolution of the hydroxide surface layer in water has been indeed observed by Mori and Draley,¹⁰ as well as by Hatcher and Rae.¹¹ Although the first authors have argued that this dissolution process plays a minor role on the corrosion behavior of aluminum in relatively short periods (up to 40 days), Hatcher and Rae have shown that this phenomenon controls the corrosion rate of aluminum when exposed for longer periods of time (1–1.5 years). In the latter case, the water in contact to the aluminum parts became turbid with time due to the precipitation into gibbsite particles of the aluminate ions (Al(OH)₄[−]) previously dissolved from the hydroxide surface layer.¹¹

The dissolution of the hydroxide layer on the surface of aluminum particles might also have occurred in the refractory castables. This hypothesis is strongly supported by the fact that the solubility of aluminum hydroxide at the usual pH range of cement-containing castables (11.5 < pH < 12.5) is 4–6 orders of magnitude higher than that observed in the pH at which the results from Mori and Draley¹⁰ and Hatcher and Rae¹¹ were obtained (Fig. 5). In fact, the dissolution of cement in the castables leads to pH values quite close to those required in the Bayer process for completely dissolving aluminum hydroxide into concentrated aluminate solutions (Bayer liquor). This explains the much faster reaction rates observed in the refractory castables in comparison to the aluminum parts used in the coolant circuits of nuclear power reactors.

3.2. Reaction kinetics

Four different stages can be identified in the H₂ generation curves depicted in Fig. 1, with the H₂ gas being predomi-

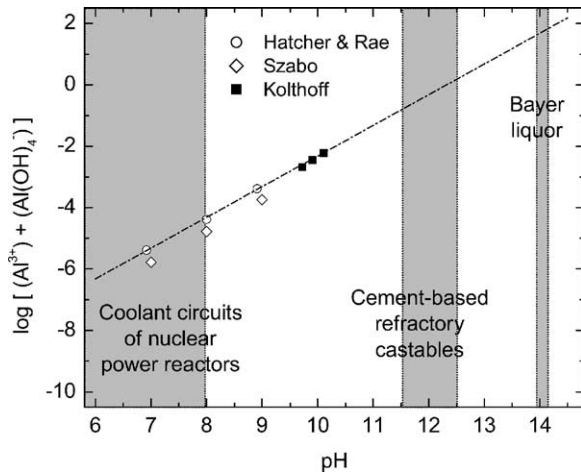


Fig. 5. Solubility diagram of aluminum hydroxide in water as a function of pH, illustrating the typical pH ranges encountered in aluminate-rich liquors of the Bayer process, cement-based refractory castables and coolant circuits of nuclear power reactors. Experimental data (symbols) were obtained from amorphous aluminum hydroxide precipitates,¹¹ whereas the dashed line was taken from the Pourbaix diagram for boehmite (AlOOH).¹⁵

nantly released during stages 2 and 3 of the process. In order to determine if the dissolution of the surface hydroxide layer is indeed the mechanism that controls the Al–H₂O reaction rate, one can attempt to correlate the kinetics of H₂ generation (Fig. 1) during stages 2 and 3 with the dissolution kinetics of Al(OH)₃ particles in water.

The dissolution rate (dW/dt) of solid particles in water is usually dependent on the residual weight of the solid (W_t), as stated by the following general equation^{12,13}

$$\frac{dW}{dt} = -k_W W_t^n \quad (5)$$

where k_W is the rate constant and n is the order of the dissolution reaction.

The reaction order n depends on the mechanism that controls the dissolution process. In the case of gibbsite particles (Al(OH)₃), Packter and Dhillon^{12,13} observed that a two-directional attack on the hexagonal platelets (in highly alkaline solutions) leads to a first-order reaction ($n = 1$), whereas a three-directional dissolution in acidic conditions renders n values of 2/3 or 4/3. The one-directional dissolution at the basal faces of gibbsite platelets would lead to zero-order reactions ($n = 0$), where the kinetics does not depend on the residual solid weight (W_t).¹²

Assuming that the stoichiometry of reactions (1)–(3) does not significantly change during the H₂ generation process, one can calculate the residual amount of Al powder in the castable as a function of time, as shown in Fig. 6. The data presented in Fig. 6 were normalized with respect to the initial Al weight W_0 and correspond to the results shown in Fig. 1 for castables containing 0.3 wt.% Al powder cured at 30 °C. The calculated curve exhibits a quite unusual weight loss profile, with a pronounced increase in the dissolution rate

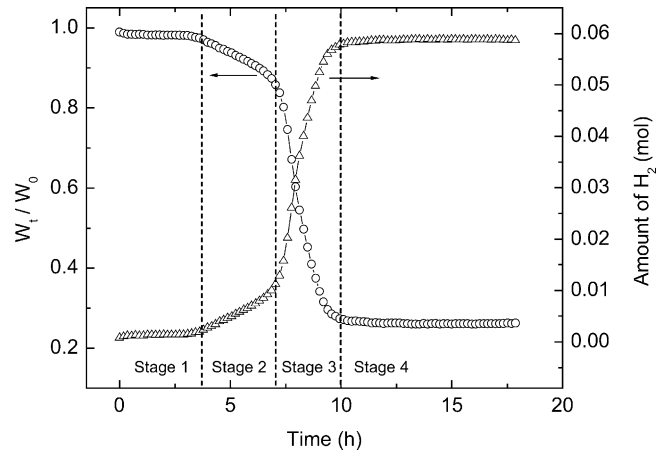


Fig. 6. Amount of residual aluminum powder (W_t/W_0) present in the castable as a function of time, assuming that the stoichiometry of reactions (1)–(3) remains constant along the H₂ generation process (results obtained for castables containing 0.3 wt.% Al powder and cured at 30 °C).

(dW/dt) on progressing from stage 2 to stage 3. Interestingly, the dissolution rate remains constant within each of these stages, indicating a zero-order dissolution reaction ($n = 0$) at the surface of the Al particles. As a result, the rate constant k_W of Eq. (5) is in this case numerically equal to the dissolution rate dW/dt .

3.3. Effect of temperature

The influence of the curing temperature on the H₂ generation process and the residual Al curves may provide additional insights on the rate-controlling step of the Al–H₂O reaction. Fig. 7 shows that the weight loss (W_t/W_0) of aluminum particles in the castable markedly changes by varying the curing temperature between 8 and 50 °C. Higher temperatures lead to faster reaction rates in both the second and third stages of the residual Al curves (Fig. 7). The effect of temperature on the kinetics of dissolution reactions is usually taken into account by assuming the following Arrhenius dependence for the rate constant k_W

$$k_W(T) = k_0 e^{-E_a/RT} \quad (6)$$

where k_0 is a constant and E_a is the activation energy of the dissolution process. Based on this equation, k_W obtained from Fig. 7 were used to assess the activation energy involved in the second and third stages of the Al–H₂O reaction.

Activation energies of 62 and 53 kJ/mol for the second and third stages, respectively, of the residual Al curves (Fig. 7) were obtained from the Arrhenius plots shown in Fig. 8. Even though the residual Al data (Fig. 7) may not be the most appropriate means to accurately determine the activation energy of the H₂ generation process, the values obtained here are comparable to those found in the literature for the dissolution of partially and totally crystallized alumina gels (gibbsite) in concentrated NaOH solutions (76 and

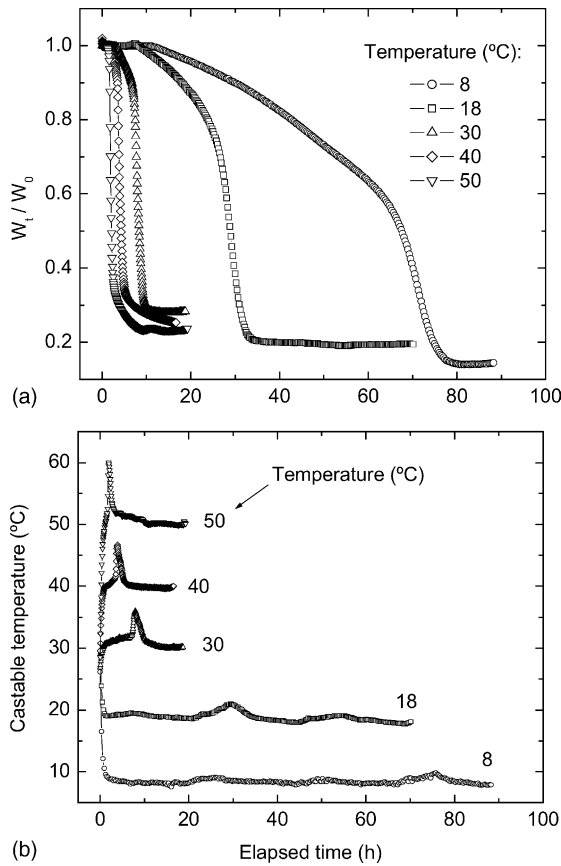


Fig. 7. Effect of curing temperature on (a) the normalized residual Al weight (W_t/W_0) and (b) the temperature of castables containing 0.3 wt.% aluminum powder (grade 101/11-NR).

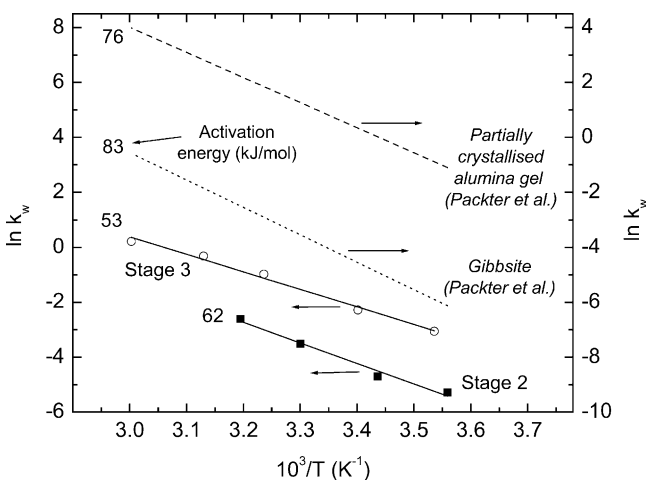


Fig. 8. Temperature dependence of the rate constant k_w at stages 2 and 3 of the Al–H₂O reaction process (see Figs. 1 and 6). The rate constants presented in this graph were calculated from the results shown in Fig. 7. The data obtained in this work for refractory castables are compared to values obtained by Packter and Dhillon¹² for the dissolution rate of totally (gibbsite) and partially crystallized alumina gel in 1 M NaOH aqueous solutions.

83 kJ/mol, respectively).¹² Contrarily, activation energies as high as 450 kJ/mol have been reported for the corrosion of aluminum plates in nuclear power plants.¹⁴ These results corroborate to the initial hypothesis that the dissolution of the protective hydroxide layer controls the kinetics of the Al–H₂O reaction in cement-containing castables.

3.4. Influence of retarding/accelerating admixtures

One aspect that still remains unclear is the reason for the presence of different stages in the H₂ evolution curves, and the relatively abrupt increase in reaction rate observed in the third stage of the Al–H₂O reaction (Figs. 1 and 7).

Fig. 7 shows that the relative amount of Al powder reacted in the second and third stages significantly depends on the castable curing temperature. Higher Al contents react in the second rather than in the third stage as the curing temperature decreases. The fact that the curing temperature strongly influences the cement dissolution and precipitation rates suggests that these processes might play an additional role on the kinetics of the Al–H₂O reaction. This supposition was evaluated by measuring the H₂ generation behavior of castables containing admixtures that either accelerate (Li₂CO₃) or retard (H₃BO₄) the dissolution/precipitation process of cement particles.

Fig. 9 reveals that the acceleration of the cement–H₂O reaction by adding Li₂CO₃ also resulted in a faster release of H₂ gas in the castables. Similarly, the addition of H₃BO₄ strongly retarded the cement dissolution/precipitation process as well as the Al–H₂O reaction. It is important to mention that although the addition of H₃BO₄ imparts a pH decrease in the castable, this effect usually does not take longer than 30–60 min, beyond which the highly alkaline conditions of cement-containing compositions prevail. These results suggest that the influence of cement on the gas generation process is not restricted solely to a pH effect; it also seems to involve the kinetics of the dissolution/precipitation reactions of cement particles in water.

3.5. Reaction mechanism

Taking into account the effects of pH, admixture and temperature described above, an attempt has been made to qualitatively describe the actual mechanism of reaction between aluminum powder and water in cement-containing refractory castables.

Assuming that the dissolution of the hydroxide layer formed on the Al particle surface controls the Al–H₂O reaction, one can use the Pourbaix diagram shown in Fig. 10 to predict the pH conditions and aluminate concentrations under which the aluminum hydroxide layer is dissolved or not from the Al surface. According to this diagram, low pH values ($6 < \text{pH} < 9$) and high aluminate concentrations would favor the stability of the hydroxide layer, protecting the Al particle from reacting with water. Alkaline pHs ($11 < \text{pH} < 14$) and low aluminate concentrations, on the other hand, would

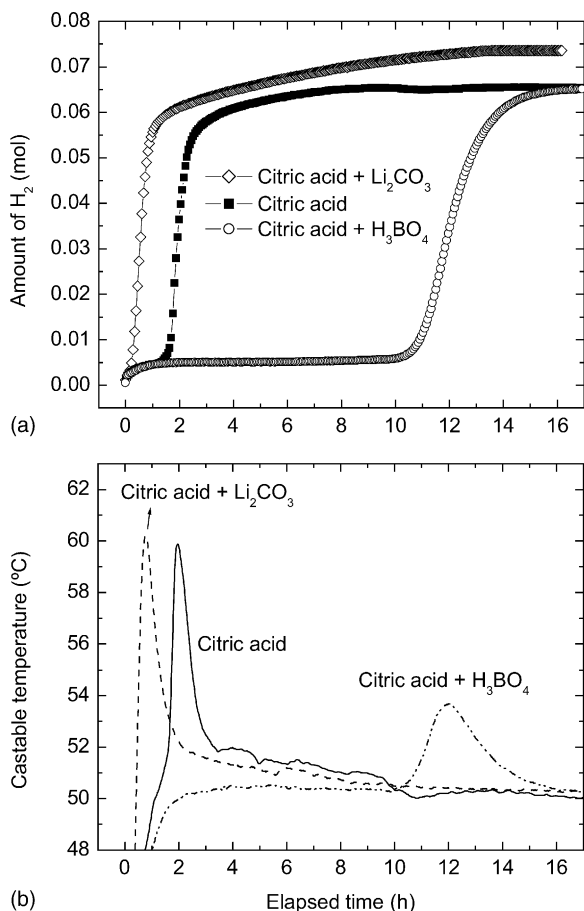


Fig. 9. Effect of accelerating (Li₂CO₃, 0.005 wt.%) and retarding (H₃BO₄, 0.10 wt.%) admixtures on (a) the amount of H₂ evolved and (b) the temperature of castables containing 0.3 wt.% aluminum powder (curing temperature: 50 °C, Al grade: 101-R). Similar results are expected for castables containing the uncoated aluminum powder grade (101/11-NR). The admixtures used were supplied by Labsynth/Brazil in anhydrous form.

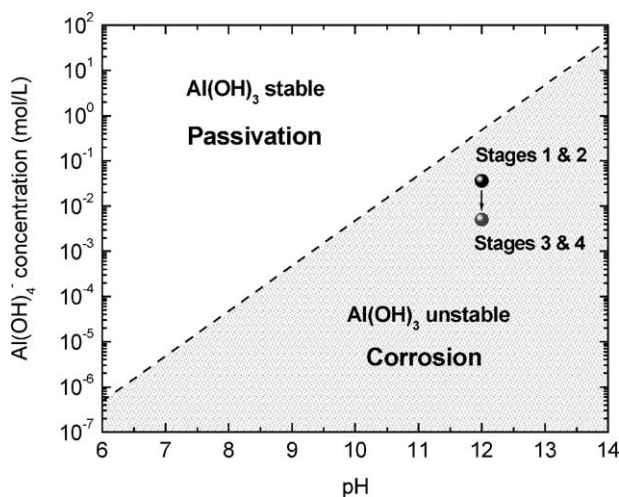
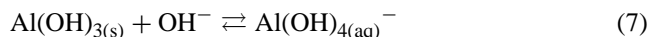


Fig. 10. Corrosion diagram of aluminum in water (25 °C) describing the conditions of pH and aluminate concentration under which the aluminum hydroxide layer (boehmite) is stable or not on the Al powder surface (adapted from Pourbaix¹⁵).

promote the dissolution of the hydroxide protective layer, exposing the Al surface to water. Once the aluminate concentration and pH values are located on the corrosion region of Fig. 10, the reaction kinetics and the thermodynamic driving force for dissolution is then determined by the distance between the actual position in the diagram and the equilibrium line that separates the corrosion from the passivation region. Therefore, larger distances would lead to faster reaction rates.

Based on this diagram, a model mechanism is suggested in Fig. 11 to describe each of the stages of the H₂ generation process in cement-based castables.

According to this model, the dissolution of the protective aluminum hydroxide layer starts already in the first stage of the process. Cement particles are expected to extensively dissolve within the first 30–60 min, increasing the pH and the concentration of Ca²⁺ and Al(OH)₄⁻ ions to a supersaturation level in the solution with respect to the calcium aluminate hydrates (Fig. 3). The fact that the concentration of Al(OH)₄⁻ ions at this condition (~0.035 mol/L) remains below the saturation level shown in the corrosion diagram (Fig. 10), leads to a continuous dissolution of the aluminum hydroxide surface layer according to the following reaction:



In spite of the onset of this reaction, H₂ is not generated within the first stage due to the presence of an aluminum hydroxide layer that keeps the aluminum inner atoms still protected from the water molecules at such early period of the process (Fig. 11).

The second stage starts when a considerable amount of the hydroxide protective layer has been dissolved from the particle surface, so that any further dissolution of the hydroxide creates sites on the surface where the aluminum metal is exposed to water. Due to its highly exothermic character, the Al–H₂O reaction occurs almost instantaneously on these sites, releasing H₂ gas and forming new Al hydroxide species at the Al–H₂O interface (see reactions (1)–(3)). It is not clear whether the Al hydroxide species formed at the interface build up a gel/solid phase on the Al surface or promptly form Al(OH)₄⁻ ions. The formation of a gel or a solid hydroxide phase on the surface is certainly favored by the locally high concentration of Al hydroxide species. In this case, the Al hydroxide gel/solid phase has to be dissolved to allow further reactions between Al and H₂O. As discussed earlier, the dissolution of this Al hydroxide layer becomes, thus, the rate-controlling step of the H₂ generation process (Fig. 8).

The transition from the second to the third stage (Fig. 11) is characterized by a considerable increase in the H₂ evolution rate, which remains approximately constant over the entire time period of the third stage. Based on the corrosion diagram (Fig. 10), such increase of the H₂ generation rate can be attributed either to a sudden pH increase or an abrupt decrease in the concentration of Al(OH)₄⁻ ions. Since no significant pH increase is expected to occur in the castable after curing

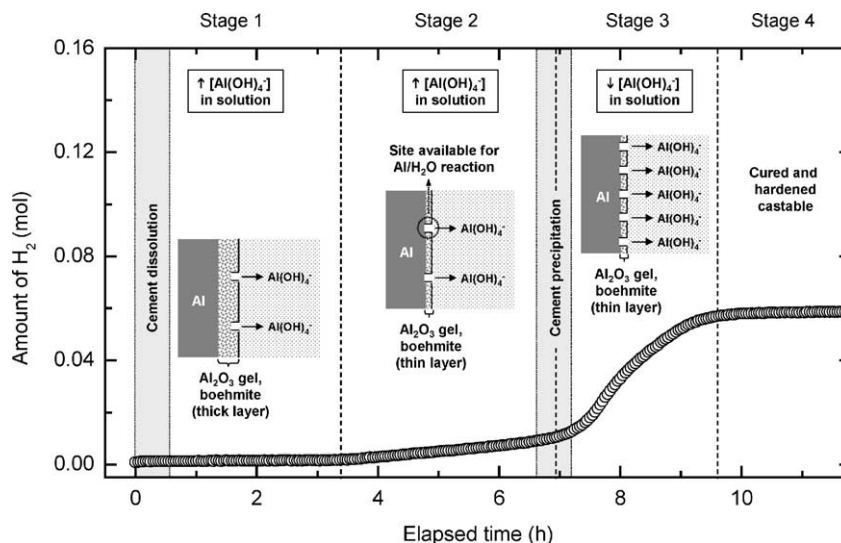


Fig. 11. Schematic diagram illustrating probable reaction mechanisms that take place during the four stages of the H_2 generation process in cement-containing refractory castables.

times from 6 to 8 h, it is very likely that the higher reaction rate observed is caused by the reduction of the concentration of $Al(OH)_4^-$ ions in solution due to the precipitation of calcium aluminate hydrates (Fig. 3). This would increase the rate at which Al reactive sites are formed on the aluminum particle surface, enhancing the H_2 generation rate until most of the aluminum powder is reacted (Fig. 11). It is worth mentioning that the temperature increase due to the precipitation of hydrates and the Al– H_2O reaction itself (Figs. 1, 4, 7 and 9), may also have contributed to increase the H_2 generation rate. However, according to the Arrhenius plots shown in Fig. 8, this temperature increase is expected to have a secondary effect on the Al– H_2O reaction rate.

Based on the model described above, one can also interpret the four different stages observed in the suspensions containing only aluminum and water (Fig. 4). The increase of the reaction rate between stages 2 and 3 could be, in this case, related to the precipitation of $Al(OH)_4^-$ ions into gibbsite particles in the solution, as previously suggested by Hatcher and Rae.¹¹ This would occur if the $Al(OH)_4^-$ ions dissolved from the Al particles achieve a supersaturation condition in the solution, favoring the precipitation of aluminum hydroxide. Further investigations would be required to check this hypothesis.

A particular feature of the Al– H_2O reaction in cement-based castables is that the $Al(OH)_4^-$ ion is involved in both of the main two reactions, namely the dissolution of the hydroxide protective layer and the dissolution/precipitation of calcium aluminate cement. Due to this particularity, the dissolution of the aluminum hydroxide surface layer is suppressed during the period when the solution is supersaturated in respect to the cement ions, leading to two distinguished reaction rates in the H_2 generation process (stages 2 and 3). If $Al(OH)_4^-$ would not be a common ion for the above-mentioned reactions, the aluminum powder

would most likely react just at the rate observed in the third stage.

Although the above model seems to be quite suitable to explain the results obtained, one should not totally discard the hypothesis that the sharp increase in reaction rate between stages 2 and 3 might also have been caused by the spalling of the oxide film layer on the surface of Al particles. Such phenomenon could be triggered by thermal stresses generated at the Al/oxide interface due to local heating at this region during the exothermic Al– H_2O reaction. This would eventually expose the Al metal directly to water and lead to an abrupt increase in the reaction rate. Additionally, one should also keep in mind that the model describes the probable mechanisms involved in the Al– H_2O reaction in a rather simplistic manner, without considering the complexity and multi-component feature of commercial cement products.

Even though some of the suggested mechanisms have still to be validated with additional experiments, we expect the present model to be useful in indicating the most important parameters that one should consider in order to deliberately control the chemical reactions that take place in Al-containing refractory castables.

Based on the model proposed, one may think of new approaches to control the Al– H_2O reaction, by manipulating the chemistry of the aqueous solution during the curing process. According to the aluminum hydroxide solubility diagram (Fig. 10), the main parameters that one may tailor to control the dissolution of the Al hydroxide surface layer and, thus, the Al– H_2O reaction are the pH and the concentration of $Al(OH)_4^-$ ions in solution. These parameters can be manipulated by properly choosing the hydraulic binders, admixtures and/or reactive powders added to the castable composition. To control the pH, for instance, one may select hydraulic binders that lead to lower/higher final pHs (e.g. reactive ρ - Al_2O_3 for lower pHs) or use chemical admixtures that would

buffer the castable pH to the desired value. The concentration of $\text{Al}(\text{OH})_4^-$ ions, on the other hand, can be manipulated by using additional sources (suppliers or consumers) of these ions in the castable composition in the form of chemical admixtures (e.g. aluminate salts) or soluble $\text{Al}(\text{OH})_3$ -containing powders (e.g. partially soluble aluminas or alumina spinels). Depending on the requirements involved (fast or low reaction rates), many possibilities may be envisaged to control the kinetics of the $\text{Al}-\text{H}_2\text{O}$ reaction based on the suggested model.

4. Conclusions

A qualitative model has been proposed in this paper to describe the reaction of aluminum powder with water in cement-based refractory castables. According to this model, the rate-limiting step of the $\text{Al}-\text{H}_2\text{O}$ reaction is in this case the dissolution of the aluminum hydroxide layer that protects the aluminum powder surface from reacting with water. The high dissolution rate of the hydroxide protective layer at the very alkaline pHs of cement-based castables is used to explain the significantly higher reaction rates observed in the castables in comparison to those that have been reported in aluminum corrosion experiments. The fact that the dissolution of aluminum hydroxide strongly depends on the concentration of aluminate ions ($\text{Al}(\text{OH})_4^-$) in solution may explain the two distinguishable $\text{Al}-\text{H}_2\text{O}$ reaction rates observed during the curing process. The lower reaction rate at earlier stages is then attributed to the high concentration of aluminate ions resulting from cement dissolution. The precipitation of the aluminate ions into calcium aluminate hydrates provides the reason for the higher reaction rate observed at a subsequent stage. The understanding of these reaction mechanisms is expected to provide insights on new approaches to control the kinetics of the $\text{Al}-\text{H}_2\text{O}$ reaction in aluminum-containing refractory castables.

Acknowledgements

The authors are grateful to Luciano A. Nascimento and Antonio E. M. Paiva (UFSCar, Brazil) for their assistance in the experimental work, to Dr. Patrick Schmutz (ETHZ,

Switzerland) for fruitful discussions, as well as to the Brazilian research funding agency FAPESP and the companies ALCOA S.A. and MAGNESITA S.A. for supporting this work.

References

- Innocentini, M. D. M., Nascimento, L. A., Paiva, A. E. M., Pandolfelli, V. C., Menegazzo, B. A. and Bittencourt, L. R. M., Aluminum-containing refractory castables, Part I: Evaluation of hydrogen gas generation. *Am. Ceram. Soc. Bull.*, 2003, **82**(6), 45–51.
- Zhang, S. and Lee, W. E., Carbon containing castables: current status and future prospects. *Br. Ceram. T.*, 2002, **101**(1), 1–8.
- Wefers, K. and Misra, C., *Oxides and Hydroxides of Aluminum: Technical Report 19—Revised*. Alcoa Laboratories, Pittsburgh, 1987, pp. 64–71.
- Alwitt, R. S., The aluminum–water system. In *Oxides and Oxide Films, Vol 4*, ed. J. W. Diggle and A. K. Vijh. Marcel Dekker, New York, 1976, pp. 170–231 (Chapter 3).
- Berzins, A., Evans, J. V. and Lowson, R. T., Aluminium corrosion studies. II—Corrosion rates in water. *Aust. J. Chem.*, 1977, **30**, 721–731.
- Foley, R. T., Localized corrosion of aluminum alloys—a review. *Corrosion*, 1986, **42**(5), 277–288.
- Innocentini, M. D. M., Studart, A. R., Pileggi, R. G. and Pandolfelli, V. C., How PSD affects the permeability of refractory castables. *Am. Ceram. Soc. Bull.*, 2001, **80**(5), 31–36.
- Studart, A. R., Zhong, W. and Pandolfelli, V. C., Rheological design of zero-cement self-flow castables. *Am. Ceram. Soc. Bull.*, 1999, **78**(5), 65–72.
- Barret, P. P., Ménétrier, D. and Bertrandie, D., Contribution to the study of the kinetic mechanism of aluminous cement setting, I—Latent periods in heterogeneous and homogeneous milieus and the absence of heterogeneous nucleation. *Cem. Concr. Res.*, 1974, **4**, 545–556.
- Mori, S. and Draley, J. E., Oxide dissolution and its effect on the corrosion of 1100 aluminum in water at 70 °C. *J. Electrochem. Soc.*, 1967, **114**(4), 352–353.
- Hatcher, S. R. and Rae, H. K., Formation and control of turbidity in aluminum–water reactor systems. *Nucl. Sci. Eng.*, 1961, **10**, 316–330.
- Packter, A. and Dhillon, H. S., Studies on recrystallised aluminum hydroxide precipitates—kinetics and mechanism of dissolution by sodium hydroxide solutions. *Colloid Polym. Sci.*, 1974, **252**, 249–256.
- Packter, A. and Dhillon, H. S., The heterogeneous reaction of gibbsite powder with aqueous inorganic acid solutions; kinetics and mechanism. *J. Chem. Soc. (A)*, 1969, 2588–2592.
- Draley, J. E., Mori, S. and Loess, R. E., The corrosion of 1100 aluminum in water from 50 °C to 95 °C. *J. Electrochem. Soc.*, 1967, **114**(4).
- Pourbaix, M., *Atlas of Electrochemical Equilibria in Aqueous Solutions (2nd English ed.)*. National Association of Corrosion Engineers, Houston, 1974, pp. 168–176 (Section 5.2, Chapter 4).